RANDOM PARAMETRIC STABILITY OF AXIALLY MOVING VISCOELASTIC PLATES UNDER NONUNIFORM, STOCHASTIC EDGE TENSION

[1]T. H. YOUNG, [2]Y. H. LI

[1,2] National Taiwan University of Science and Technology, of Science and Technology
E-mail:[1]thyoung@mail.ntust.edu.tw, [2]m10303145@mail.ntust.edu.tw

Abstract - This paper investigates the random parametric stability of an axially moving web subjected to a pair of nonuniformly distributed, stochastic edge tension on two opposite, simply-supported edges. The web is modeled as a viscoelastic plate whose const itutive relation obeys the Kelvin- Voigt model, and the edge tension is expressed as the sum of a static tension and a random process with a zero mean. Due to the random edge tension, the moving plate may bring about parametric random instability under certain situations. Numerical results show that an increase in the resultant of the stochastic part of the edge tension will reduce the stable region of the plate, but the distribution form of the stochastic part of the edge tension has a minor effect on the stability of the plate.

Index Terms - Axially Moving Viscoelastic Plate, Nonuniform Edge Tension, Stochastic Averaging Method, Random Stability.

I. INTRODUCTION

Axially moving webs are frequently encountered in industrial applications, such as magnetic tapes, transmission belts, paper webs, plastic sheets, band saw blades, etc. The performance of axially moving webs depends largely on their dynamic behaviors; therefore, hundreds of references pertaining to the dynamic behaviors of axially moving webs can be found in the literature. Based on the aspect ratio of the axially moving webs between two adjacent supports, they can be regarded as one- dimensional structures or two-dimensional structures. Furthermore, according to the flexural rigidity of the axially moving webs, they can be modeled as strings [1]-[2] or beams [3] for webs with large aspect ratios and as membranes [4]-[5] or plates [6]-[7] for webs with small aspect ratios.

According to previous experiences, the moving speed and the tension are two major factors which influence the dynamic behaviors of axially moving webs. Earlier researchers deal mainly with the determination of the critical speed of the webs axially moving with constant speeds and subjected to static, uniformly distributed tensions. However, recent researches focus primarily on the dynamic response and stability of the axially moving webs under various complicated effects, such as nonconstant moving speeds, time-dependent and/or nonuniformly distributed tensions, etc. In reality, the moving speed and the applied tension of the axially moving web are generally time-dependent. Due to the time-dependent moving speed or tension, the axially moving web may experience parametric instability before the moving speed of the web exceeds its first critical speed. Chen and Yang [8] investigated the nonlinear response at principal parametric resonances for viscoelastic beams moving with axial pulsating speed. The pulsating speed of the moving beam is assumed to be the sum of a constant speed and a small, harmonically varying perturbation, and the material property of the viscoelastic beam obeys the Kelvin model. Marynowski [9] studied the nonlinear vibration of axially moving viscoelastic beams with a constant speed and subjected to a time-dependent tension. The time-dependent tension is assumed to a small, harmonically varying perturbation superimposed on a steady-state tension, and the internal damping of the viscoelastic beam is introduced by the Kelvin-Voigt model. Tang and Chen [10] analyzed the parametric instability of axially moving viscoelastic plates with time-dependent speeds.

The time-dependent speed of the moving plate is assumed to be the sum of a constant speed and a small, harmonically varying perturbation, and the tension is assumed to be uniformly distributed on two opposite edges. Liu [11] investigated the dynamic stability of an axially moving web which translates with periodically varying speeds and is subjected to partially distributed tensions on two opposite simply-supported edges. The web is modeled as a viscoelastic rectangular plate which obeys the Kelvin-Voigt model. The moving speed of the plate is expressed as the sum of a constant speed and a periodical perturbation. Dynamic instability of a moving plate subjected to uniformly distributed parametric in-plane forces was analyzed by Lengoc and Mccallion [12]. The extended Galerkin method is used to discretize the differential equation of motion, and the harmonic balance method is employed for investigating the unstable regions of the moving plate. Chiu [13] investigated the parametric stability of an axially moving web subjected to nonuniform in-plane

edge excitations on two opposite, simply-supported edges. The web is modeled as a viscoelastic plate whose constitutive relation obeys the Kelvin-Voigt model, and the in-plane edge excitations are expressed as the sum of a static tension and a periodical perturbation.

As far as authors' knowledge, very few researches on stochastic behavior of axially moving webs are reported in the literature. Therefore, this paper investigates the random parametric stability of an axially moving web subjected to a pair of nonuniformly distributed, stochastic edge tension on two opposite, simply-supported edges.

II. EQUATIONS OF MOTION

Consider a rectangular plate of dimension $a \times b$ moving in the x-direction with a constant speed V. The plate is simply supported on two opposite edges $x = 0$ and a, and is free on the other two edges $y = 0$ and b. The plate is subjected to a random excitation $f(\mathrm{y,t})$ arbitrarily distributed on two simply supported edges, as shown in Fig. 1. The plate possesses an internal damping of which the constitutive relation obeys the Kelvin-Voigt model, i.e.,

$$\sigma = E(\varepsilon + c\frac{\partial \varepsilon}{\partial t}) \tag{1}$$

where σ and ε are the stress and strain of the plate, respectively, and t is the temporal variable. E and c are Young's modulus and internal damping coefficient of the plate, respectively.

The equation of motion for the lateral vibration of such a plate can be written as

$$\rho h(\frac{\partial^2 w}{\partial t^2} + 2V\frac{\partial^2 w}{\partial t \partial x} + V^2\frac{\partial^2 w}{\partial x^2}) + (1 + c\frac{\partial}{\partial t})D\nabla^4 w = \frac{\partial}{\partial x}(N_{xx}\frac{\partial w}{\partial x}) + \frac{\partial}{\partial y}(N_{yy}\frac{\partial w}{\partial y}) + \frac{\partial}{\partial x}(N_{xy}\frac{\partial w}{\partial y}) + \frac{\partial}{\partial y}(N_{xy}\frac{\partial w}{\partial x}) \tag{2}$$

where w and D are the lateral displacement and the flexural rigidity of the moving plate, respectively. ρ and h are the mass density and the thickness of the plate, respectively. ∇^4 is a Laplacian operator in Cartesian coordinates. N_{xx}, N_{yy}, and N_{xy} are the in-plane stress resultants of the plate. Equation (2) is the same as that appeared in literature [6]-[7]. The boundary conditions for the lateral vibration of the moving plate are as follows,

at $x = 0$ and a, $w = 0$ and $\frac{\partial^2 w}{\partial x^2} = 0$, (3a)

at $\mathrm{y} = 0$ and b, $\frac{\partial^2 w}{\partial y^2} = 0$ and $\frac{\partial^3 w}{\partial y^3} + (2-\nu)\frac{\partial^3 w}{\partial y \partial x^3} = 0$, (3b)

where ν is Poisson's ratio of the plate.

To analyze the lateral dynamic behavior of the plate, the in-plane stress resultants N_{xx}, N_{yy}, and N_{xy} due to edge excitation $f(y,t)$ have to be found first. If the plate is thin such that the lowest natural frequency of the in-plane vibration is much higher than that of the out-of-plane vibration of the plate, the effect of the in-plane inertia can be neglected in determining the in-plane stress resultants without causing any significant errors. Therefore, the spatial distribution of the in-plane stress resultants can be obtained by solving the following in-plane static equilibrium problem,

$$\frac{\partial N_{xx}}{\partial x} + \frac{\partial N_{xy}}{\partial y} = 0, \tag{4a}$$

$$\frac{\partial N_{xy}}{\partial x} + \frac{\partial N_{yy}}{\partial y} = 0, \tag{4b}$$

with boundary conditions

$N_{xx} = f_1(\mathrm{y})$ and $v = 0$, at $x = 0$ and a,

$N_y = 0$ and $N_{xy} = 0$, at $\mathrm{y} = 0$ and b,

where v is the in-plane transverse displacement of the plate, and the edge excitation is expressed as $f(\mathrm{y,t}) = f_1(y)\,f_2(t)$. The actual in-plane stress resultants due to the random excitation $f(y,t)$ are then determined approximately by multiplying the in-plane stress resultants obtained by this static problem with $f_2(t)$.

The above in-plane static equilibrium problem is not easy to solve when the edge tensions are not uniformly distributed on two opposite edges. However, one can obtain an approximate solution of the problem in terms of in-plane displacements u and v by various approximate methods. Due to the boundary conditions of the problem, it is very difficult to find a set of comparison functions as trial functions. Therefore, the extended Ritz method, which admits admissible functions as trial functions, is adopted in conjunction with the Hamilton principle,

$$\delta(U - W_k) = 0, \tag{5}$$

where U and W_k are the in-plane strain energy of the ing plates and the work done by the static edge tension $f_1(y)$, respectively,

Assume the in-plane displacement components u and v to be of the forms,

$$u(x,y) = \sum_{m=0}^{M}\sum_{n=0}^{N} A_{mn}(\frac{x}{a})^m(\frac{y}{b})^n \tag{6a}$$

$$v(x,y) = \sum_{m=0}^{M}\sum_{n=0}^{N} B_{mn}\sin(\frac{(m+1)\pi x}{a})(\frac{y}{b})^n \tag{6b}$$

where A_{mn} and B_{mn} are undetermined coefficients. The assumed displacements satisfy the only geometric boundary condition $v = 0$ at the edges $x = 0$ and a. Substituting the assumed the in-plane displacements into (5) yields the following system equations,

$$[K_i]X_i = F_i\,, \tag{7}$$

where $[K_i]$ is the stiffness matrix of in-plane deformation, F_i is the force column matrix, and X_i is the column matrix formed by all A_{mn} and B_{mn} Solving the above system equations for all A_{mn} and B_{mn}, the in-plane displacements u and v are determined, so are the in-plane stress resultants N_{xx}, N_{yy}, and N_{xy} by the constitutive relationship of the in-plane stress problem.

Having the expressions for the in-plane stress resultants, we are ready to solve the lateral vibration of such a plate. Because (2) is a fourth order partial differential equation with variable coefficients, it is unable to be solved directly. Therefore, dependence on spatial coordinates is eliminated first, and the equation is transformed into an ordinary differential equation. Since expressions for in-plane stress resultants are very messy, it is impossible to find the solution for (2). Therefore, approximate methods are utilized again to obtain discretized system equations for the equation. In this work, the extended Galerkin method with simpler trial functions is adopted.

Assume the transverse displacement w as

$$w=\sum_{k=1}^{K}\sum_{l=0}^{L}C_{kl}(t)\sin(\frac{k\pi}{a}x)(\frac{y}{b})^l \tag{8}$$

where $C_{kl}(t)$ are undetermined functions. The assumed displacement satisfies the boundary conditions at both simply supported edges $x=0$ and a, but it does not satisfy the boundary conditions at both free edges $y=0$ and b. On substituting the assumed displacement into the out-of-plane equation and the boundary conditions yields certain residues. The extended Galerkin method requires the overall residue weighted by the trial functions vanish, i.e.,

$$\int_0^b\int_0^a \gamma\sin(\frac{k\pi}{a}x)(\frac{y}{b})^l dxdy+\int_0^a V_y\sin(\frac{k\pi}{a}x)(\frac{y}{b})^l\Big|_{y=0,b}dx$$

$$-\int_0^a M_{yy}\sin(\frac{k\pi}{a}x)(\frac{d}{dy}(\frac{y}{b})^l)\Big|_{y=0,b}dx=0 \tag{9}$$

where γ, V_y and M_{yy} are residues of the out-of-plane equation, transverse shear resultants and bending moment resultants along the free edges, respectively. Substituting the assumed displacement w into (9) and non- dimensionalizing all parameters yield the following equation,

$$[M_0]W''+(\bar{V}[G_o]+\tilde{c}[K_{oe}])W'+([K_{oe}]+\bar{V}^2[K_{og}]+[F_o])W$$
$$=-p(\tau)[F_o]W \tag{10}$$

where the nondimensional parameters

$$\bar{V}=V\sqrt{\frac{\rho hb^2}{D}},\quad \tilde{c}=c\sqrt{\frac{D}{\rho hb^4}},\quad \tau=t\sqrt{\frac{D}{\rho hb^4}},$$

$p(\tau)$ is a random process with a zero mean such that $f_2(\tau)=1+p(\tau)$ is assumed, and a prime denotes a differentiation with respect to τ. The mass matrix $[M_0]$, the elastic stiffness matrix $[K_{oe}]$, the geometric stiffness matrix $[K_{og}]$ and the force matrix $[F_o]$ are symmetric, while the gyroscopic matrix $[G_o]$ is skew-symmetric. The displacement vector W is a column matrix formed by all undetermined functions $C_{kl}(\tau)$.

Equation (10) is a set of simultaneous second-order differential equations with periodic coefficients, of which an analytic solution is still hard to find. To improve the solvability, a modal analysis suitable for gyroscopic systems is conducted to partially uncouple terms on the left-hand side of the equation. First define a state vector

$$q=\begin{bmatrix}W'\\W\end{bmatrix},\text{ and rewritten (10) as}$$

$$\begin{bmatrix}[M_0] & [0]\\ [0] & [K_o]\end{bmatrix}q'+\begin{bmatrix}\bar{V}[G_o] & [K_o]\\ -[K_o] & [0]\end{bmatrix}q$$
$$=-\tilde{c}\begin{bmatrix}[K_{oe}] & [0]\\ [0] & [0]\end{bmatrix}q-p(\tau)\begin{bmatrix}[0] & [F_o]\\ [0] & [0]\end{bmatrix}q \tag{11}$$

where $[K_o]=[K_{oe}]+\bar{V}^2[K_{og}]+[F_o]$. Next consider the eigenvalue problem of the corresponding free, undamped gyroscopic system. The eigenvalue of the gyroscopic system s appears in pure imaginary pairs, $s=\pm i\omega_n$, n=1, 2, …, J, where $J=K\times L$ is the total degrees of freedom of the discretized system, and the corresponding eigenvector Q appears in complex conjugate pairs, $Q=X_n\pm iY_n$. By the orthogonality of the eigenvectors, some matrices in (11) can be diagonalized by the modal matrix $[P]$, i.e.,

$$[P]^T\begin{bmatrix}[M_o] & [0]\\ [0] & [K_o]\end{bmatrix}[P]=[I],\ [P]^T\begin{bmatrix}\tilde{V}[G_o] & [[K_o]]\\ -[[K_o]] & [0]\end{bmatrix}[P]=[\Lambda] \tag{12}$$

where $[P]^T$ is the transpose of [P], [I] is an identity matrix, and $[\Lambda]$ is a block-diagonal matrix of the form

$$[\Lambda]=diag.\begin{bmatrix}0 & -\omega_r\\ \omega_r & 0\end{bmatrix}.$$

Then, introduce a linear transformation $q=[P]\varsigma$, Upon substituting this transformation into (11) and pre- multiplying $[P]^T$ to the equation yields

$$\varsigma'+[\Lambda]\varsigma=-\tilde{c}[C]\varsigma-p(\tau)[F]\varsigma, \tag{13}$$

where the matrices

$$[C]=[P]^T\begin{bmatrix}[K_{oe}] & [0]\\ [0] & [0]\end{bmatrix}[P],\text{ and }[F]=[P]^T\begin{bmatrix}[0] & [F_o]\\ [0] & [0]\end{bmatrix}[P].$$

Note that the matrix [C] is again symmetric since $[K_{oe}]$ is symmetric. The terms on the left-hand side of the above equation are uncoupled in a block sense;

however, those on the right-hand side are still coupled. To match the form of the matrix $[\Lambda]$, matrices on the right-hand side of the equation are partitioned into $J\times J$ pieces of 2×2 blocks. Therefore, the above equation can be rewritten as

$$\xi' - \omega_n\eta_n = -\tilde{c}\sum_{m=1}^{I}\left(\alpha_{nm}^{11}\xi_m + \alpha_{nm}^{12}\eta_m\right) - p(\tau)\sum_{m=1}^{J}\left(h_{nm}^{11}\xi_m + h_{nm}^{12}\eta_m\right)$$

(14a)

$$\eta' - \omega_n\xi_n = -\tilde{c}\sum_{m=1}^{I}\left(\alpha_{nm}^{21}\xi_m + \alpha_{nm}^{22}\eta_m\right) - p(\tau)\sum_{m=1}^{J}\left(h_{nm}^{21}\xi_m + h_{nm}^{22}\eta_m\right)$$

n=1, 2, …,J (14b)

where α_{nm}^{rs} and h_{nm}^{rs} are the r-sth entries of the n-mth block of the matrices [C] and [F], respectively. ξ_n and η_n are the (2n-1)th and the 2nth entries of ς. The above pair of equations is coupled, stochastic differential equations and is very difficult to solve. But if terms on the right-hand side of the equation are small in certain senses as compared with those on the left-hand side, stochastic average method can be used to find an analytic solution.

III .STOCHASTIC AVERAGING METHOD

Assume the solutions of (14) as

$$\xi_n = z_n e^{i\omega_n\tau} + \overline{z}_n e^{-i\omega_n\tau}, \quad (15a)$$

$$\eta_n = i\left(z_n e^{i\omega_n\tau} - \overline{z}_n e^{-i\omega_n\tau}\right), \quad \text{n=1, 2, …., J} \quad (15b)$$

where z_n and $\overline{z}_n$ are complex conjugate responses of the system. Substituting (15) into (14), one can solve for z_n,

$$\dot{z}_n = \tilde{c}q_n\left(z_n,\overline{z}_n;\tau\right) + p(\tau)g_n\left(z_n,\overline{z}_n;\tau\right)$$

n=1, 2, …., J (16)

If the damping factor $\tilde{c}$ and the random excitation $p(\tau)$ are small in some senses such that $\tilde{c}$ is of order ε, and $p(\tau)$ is of order $\varepsilon^{1/2}$, the stochastic averaging procedure can be applied to (16), and z can be uniformly approximated in the weak sense by a Markov vector [14], i.e.,

$$dz_n = m_n d\tau + \sum_{r=1}^{J}\sigma_{nr}dB_r, \quad \text{n=1, 2, …., J} \quad (17)$$

where B_r are mutually independent unit Wiener process; m_n are drift coefficients, and σ_{nr} are the n-rth element of the diffusion matrix $[\sigma]$.

By Ito's differential rule [14], the Ito differential equation for $z_n\overline{z}_n$ can be derived as

$$\begin{aligned}\mathrm{d}\left(z_n\overline{z}_n\right) = \Big\{&-\tilde{c}\left(\alpha_{nn}^{11}+\alpha_{nn}^{22}\right) + \frac{1}{8}\sum_{r=1}^{J}\Big[\left(h_{rn}^{11}+ih_{rn}^{12}-ih_{rn}^{21}\right.\\ &\left.+h_{rn}^{22}\right)\left(h_{nr}^{11}+ih_{nr}^{12}-ih_{nr}^{21}+h_{nr}^{22}\right)\left(S\left(\omega_n-\omega_r\right)-i\psi\left(\omega_n\right.\right.\\ &\left.\left.-\omega_r\right)\right)+\left(h_{rn}^{11}+ih_{rn}^{12}+ih_{rn}^{21}-h_{rn}^{22}\right)\left(h_{nr}^{11}-ih_{nr}^{12}-ih_{nr}^{21}\right.\\ &\left.-h_{nr}^{22}\right)\left(S\left(\omega_n+\omega_r\right)-i\psi\left(\omega_n+\omega_r\right)\right)+\left(h_{rn}^{11}-ih_{rn}^{12}+ih_{rn}^{21}\right.\\ &\left.+h_{rn}^{22}\right)\left(h_{nr}^{11}-ih_{nr}^{12}-ih_{rn}^{21}-h_{rn}^{22}\right)\left(h_{nr}^{11}+ih_{nr}^{12}+ih_{nr}^{21}\right.\\ &\left.-h_{nr}^{22}\right)\left(S\left(\omega_n+\omega_r\right)+i\psi\left(\omega_n+\omega_r\right)\right)\Big]+\frac{1}{4}\Big[\left(h_{nn}^{11}+ih_{nn}^{12}\right.\\ &\left.-ih_{nn}^{21}+h_{nn}^{22}\right)\left(h_{nn}^{11}-ih_{nn}^{12}+ih_{nn}^{21}+h_{nn}^{22}\right)S(0)+\left(h_{nn}^{11}\right.\\ &\left.-ih_{nn}^{12}-ih_{nn}^{21}-h_{nn}^{22}\right)\left(h_{nn}^{11}+ih_{nn}^{12}+ih_{nn}^{21}\right.\\ &\left.-h_{nn}^{22}\right)S\left(2\omega_n\right)\Big]\Big\}z_n\overline{z}_n\mathrm{d}\tau+\sum_{r=1}^{2J}\left(\sigma_{nr}\overline{z}_n+\sigma_{(n+J)r}z_n\right)\mathrm{d}B_r\end{aligned}$$

n=1, 2, …, J, (18)

where $S(\omega)$ and $\psi(\omega)$ are the real and imaginary parts of the spectral density function of $p(\tau)$, i.e.,

$$S(\omega) = 2\int_0^\infty R(\tau)\cos\omega\tau\,\mathrm{d}\tau, \quad \psi(\omega) = 2\int_0^\infty R(\tau)\sin\omega\tau\,\mathrm{d}\tau$$

.

Taking the ensemble average of (18) yields the second- moment equation for the mean-square response of the system. It is evident that the resulting equation will be the same as (18) with the stochastic terms being absent and the response variables $z_n\overline{z}_n$ replaced by their expectations, and the second –moment equation can be written as

$$\frac{d}{d\tau}Z = [B]Z \quad ,$$

(19)

where $Z = \left\{E\left[z_n\overline{z}_n\right], E\left[z_n\overline{z}_n\right],\ldots,E\left[z_n\overline{z}_n\right]\right\}^T$, and [B] is a constant coefficient matrix. The second-moment stability of the system is assured if the mean-square response of the system Z is bounded, which demands that the real parts of all eigenvalues of [B] be negative. Consequently, the second-moment stability criterion corresponds to the one that first renders the real part of an eigenvalue of [B] being 0.

IV.NUMERICAL RESULTS AND DISCUSSIONS

As an application of the general solution, the random process $p(\tau)$ used to produce numerical results in this section is assumed as a Gaussian white noise with a spectral density S for simplicity, i.e., $S(0)=S(2\omega_n)=S(\omega_n\pm\omega_r)=S$, and $\psi(\omega_n\pm\omega_r)=0$. However, numerical results for other random processes can be also generated easily. Fig. 2 shows the second-moment stability boundaries of axially moving plates of different aspect ratios subjected to uniformly distributed in-plane edge excitation. In this case, the edge excitation $f(y,t)=f_0\left[1+p(t)\right]$, and the non- dimensional mean intensity $\tilde{f}_0 = f_0b^2/D$. The second- moment stability boundaries on the $S-\tilde{c}$ plot is a straight line originated from the origin

because all the entries of the coefficient matrix [B] in (19) are functions of the ratio $S/\tilde{c}$ for a Gaussian white noise excitation $p(\tau)$. The unstable region lies above the stability boundary. It means that a stronger random edge excitation or a lighter internal damping will make the system unstable. Therefore, the effect of the internal damping of the plate is stabilizing, while the effect of the random part of the edge tension is destabilizing. As the aspect ratio a/b of the plate increases, the stability boundary becomes less steeper, leaving a larger unstable region. This may be attributed to the fact that the plate is simply supported only on two opposite axial edges; hence, the plate becomes more flexible as this aspect ratio increases. Consequently, the effect of the aspect ratio a/b of the plate is destabilizing. Since the second-moment stability boundary on the $S-\tilde{c}$ plot is a straight line originated from the origin, as shown in the above figure, it depends only on the ratio $S/\tilde{c}$. The stability boundary is plotted versus this ratio hereafter. Fig. 3 presents the second-moment stability boundaries of axially moving square plates with different moving speeds subjected to uniformly distributed in-plane edge excitation. The Unstable region of the system lies above the stability boundary. All stability boundaries are quite low and flat for large mean intensity of the edge tension and become very high and steep as the mean intensity gets smaller. This is because a larger mean intensity of the edge tension is accompanied with a stronger random excitation. These stability boundaries shift to the left and leave larger unstable regions as the moving speed increases because all natural frequencies of the plate decrease as the moving speed increases. Therefore, the effect of moving speed is destabilizing. When the value of mean edge tension exceeds a certain value, all stability boundaries almost coalesce together, which means that the effect is no longer significant as compared with the effect of the random edge tension. The second-moment stability boundaries of axially moving plates subjected to uniformly distributed in-plane edge excitation of different mean intensities are depicted in Fig. 4. The aspect ratio a/b in Fig. 4(a) is 2, and is $1/2$ in Fig. 4(b). In Fig. 7(a), each stability boundary starts from a point on the ordinate. The smaller the mean intensity of the edge excitation is, the larger the $S/\tilde{c}$ value of the point is. As the moving speed increases, each stability boundary rises and reaches a peak in order as the mean intensity of the edge excitation. As the moving speed further increases, all the stability boundaries lower and meet the abscissa in order as the mean intensity of the edge excitation. Beyond these critical speeds, the plate is unstable even in the absence of randomness of the edge tension. In Fig. 4(b), each stability boundary starts also from a point, whose $S/\tilde{c}$ value is in reverse order as the mean intensity of the edge excitation. As the moving speed increases, all the stability boundaries lower without any peaks. The smaller the mean intensity of the edge excitation is, the steeper the stability boundary is. Finally, all the stability boundaries meet the abscissa in order as the mean intensity of the edge excitation. Beyond these critical speeds, the plate is unstable even in the absence of randomness of the edge tension. Comparing between these two figures, it is found that the $S/\tilde{c}$ values of the stability boundary of the plate with aspect ratio a/b = 2 are much smaller than those having aspect ratio $a/b = 1/2$ because the effect of the aspect ratio a/b of the plate is destabilizing as above-mentioned.

Fig. 5 illustrates the second-moment stability boundaries of axially moving plates subjected to different spatial distributions of the in-plane edge excitation having the same resultant. The aspect ratio a/b in Fig. 5(a) is 2, and is $1/2$ in Fig. 5(b). In Fig. 5(a), all three stability boundaries, which are subjected to uniform, linear and quadratic distributions, respectively, rise and then lower as the moving speed increases, leaving a peak for each stability boundary at about the same moving speed. All three stability boundaries almost coalesce together except in the neighborhood of peaks where a small difference between the stability boundary subjected to quadratic distribution and the stability boundaries subjected to uniform and linear distributions is observed. In Fig. 5(b), all three stability boundaries lower without any peaks as the moving speed increases. The stability boundaries which are subjected to uniform and linear distributions almost coalesce together, and are a little bit lower than that subjected to quadratic distribution. The higher the moving speed is, the smaller the difference between these stability boundaries is. Comparing between these two figures, it is observed that the effect of spatial distribution of the in-plane edge excitation is more profound for a plate with smaller aspect ratio a/b than for a plate with larger aspect ratio. But the effect of spatial distribution of the in-plane edge excitation is much less significant than that of the mean resultant of the edge tension, as shown in Fig. 3.

CONCLUSIONS

From the above numerical results, the following conclusions can be drawn:

1. The second-moment stability boundary of the axially moving plate on the $S-\tilde{c}$ plot is a straight line originated from the origin, and the stability boundary depends only on the ratio $S/\tilde{c}$ if the random part of the edge tension is a Gaussian white noise.

2. The effect of the random part of the edge tension is destabilizing, but the effect of spatial distribution of the random edge tension is much less significant than that of the mean resultant of the edge tension. The effect of spatial distribution of the random edge excitation is more profound for a plate with smaller aspect ratio a/b than for a plate with larger aspect ratio.
3. The effect of the aspect ratio a/b of the plate is destabilizing, so is the effect of the moving speed. However, the effect the moving speed is less important as the effects of the random edge tension and the aspect ratio. But when the moving speed exceeds the critical speed, the plate becomes unstable even in the absence of randomness of the edge tension.
4. The effect of the internal damping is stabilizing.

REFERENCES

[1] F. Fung, J. S. Huang, and Y. C. Chen, "The transient amplitude of the viscoelastic travelling string: An integral constitutive law," Journal of Sound and Vibration, vol. 201, pp. 153-167, 1997.

[2] L. Q. Chen, W. J. Zhao, and J. W. Zu, "Transient response of an axially accelerating viscoelastic string constituted by a functional differential law," Journal of Sound and Vibration, vol. 278, pp. 861-871, 2004.

[3] L. Q. Chen, Y. Q. Tang, and C. W. Lim, "Dynamic stability in parametric resonance of axially accelerating viscoelastic Timoshenko beams," Journal of Sound and Vibration, vol. 329, pp. 547-565, 2010.

[4] M. Marynowski, "Two-Dimensional rheological element in modeling of axial moving viscoelastic web," European Journal of Mechanics A/Solids, vol. 25, pp. 729-744, 2006.

[5] C. Shin, J. Chung, and H. Heeyoo, "Dynamic responses of the in-plane and out-of-plane vibrations for an axially moving membrane," Journal of Sound and Vibration, vol. 297, pp. 794-809, 2006.

[6] C. C. Lin, "Stability and vibration characteristics of axially moving plates," International Journal of Solids and Structures, vol. 34, pp. 3179-3190, 1997.

[7] N. Banichuk, J. Jeronen, P. Neittaanmaki, and T. Tuovinen, "On the instability of an axially moving elastic plate," International Journal of Solids and Structures, vol. 47, pp. 91-99, 2010.

[8] L. Q. Chen, and X. D. Yang, "Steady-State response of axially moving viscoelastic beams with pulsating speed: Comparison of two nonlinear models," International Journal of Solids and Structures, vol. 42, pp. 37-50, 2005.

[9] M. Marynowski, "Non-Linear vibrations of an axially moving viscoelastic web with time-dependent tension," Chaos, Solitons & Fractals, vol. 21, pp. 481-490, 2010.

[10] Y. Q. Tang, and L. Q. Chen, "Stability analysis and numerical confirmation in parametric resonance of axially moving viscoelastic plates with time-dependent speed," European Journal of Mechanics A/Solids, vol. 37, pp. 106-121, 2013.

[11] C. Liu, Dynamic Stability of Axially Moving Viscoelastic Plates with Pulsating Speeds and Nonuniform Edge Tensions, Master Thesis, National Taiwan University of Science and Technology, 2011 (in Chinese).

[12] L. Lengoc, and H. Mccallion, "Wide bandsaw blade under cutting conditions, Part II: Stability of a plate moving in its plane while subjected to parametric excitation," Journal of Sound and Vibration, vol.186, pp. 143-162, 1995.

[13] Y. S. Chiu, Dynamic Stability of Axially Moving Viscoelastic Plates under and Nonuniform Edge Excitations, Master Thesis, National Taiwan University of Science and Technology, 2013 (in Chinese).

[14] Y. K. Lin, and G. Q. Cai, Probabilistic Structural Dynamics, McGraw-Hill, Inc., New York, 1995.

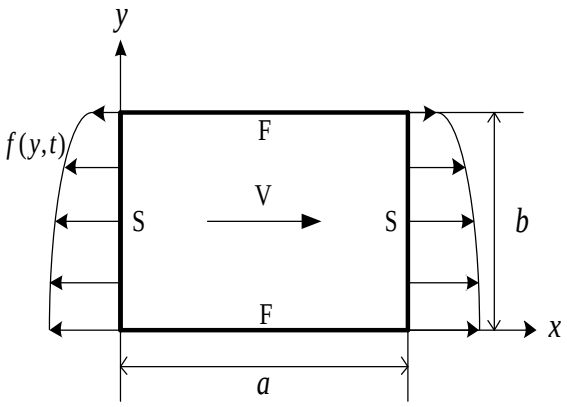


Fig. 1. A rectangular plate of dimension $a \times b$ moving in the x-direction with a constant speed V and subjected to a random edge excitation $f(y,t)$.

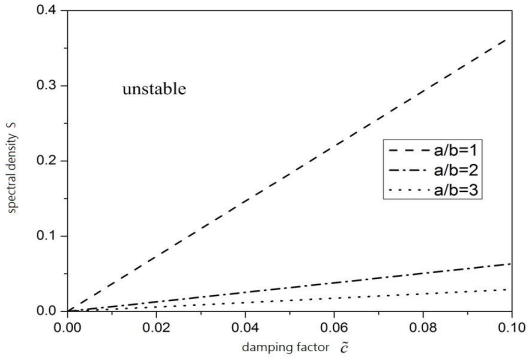


Fig. 2. The second-moment stability boundaries of axially moving plates of different aspect ratios subjected to uniformly distributed in-plane edge excitation. $\tilde{V} = 1.0$ and $\tilde{f}_0 = 10$.

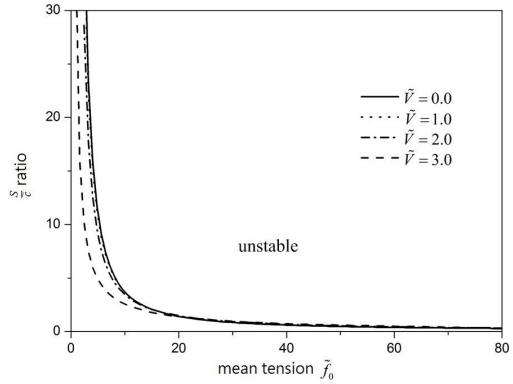
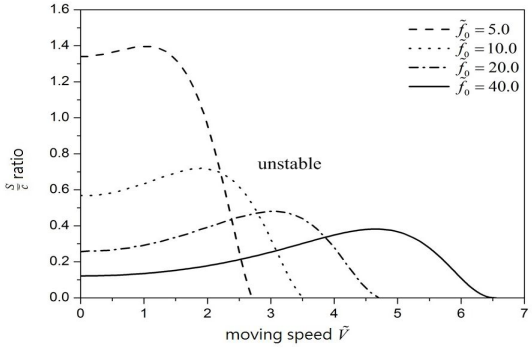
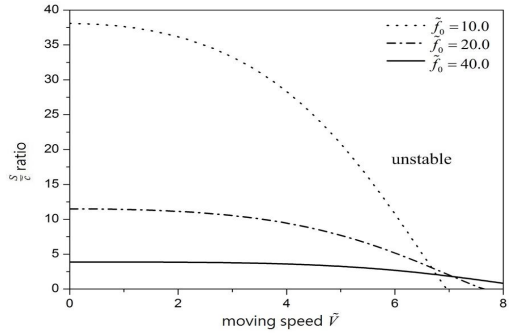


Fig. 3. The second-moment stability boundaries of axially moving square plates with different moving speeds subjected to uniformly distributed in-plane edge excitation.

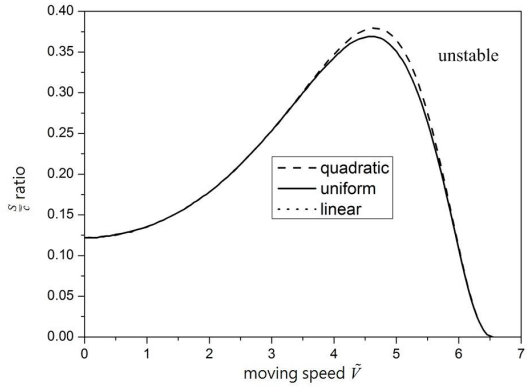


(a) $\frac{a}{b}=2$

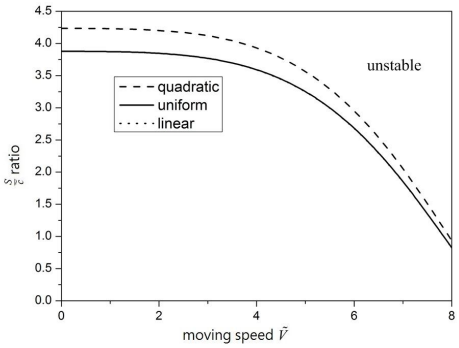


(b) $\frac{a}{b}=\frac{1}{2}$

Fig. 4. The second-moment stability boundaries of axially moving plates subjected to uniformly distributed in-plane edge excitation of different mean intensities.



(a) $\frac{a}{b}=2$



(b) $\frac{a}{b}=\frac{1}{2}$

Fig. 5. The second-moment stability boundaries of axially moving plates subjected to uniformly distributed in-plane edge excitation of different mean intensities. $\tilde{f}_0=40$.

★★★